



Main factors influencing the formation of thermogenic solid bitumen

Rui Lei^{a,b}, Yongqiang Xiong^{a,*}, Yun Li^a, Li Zhang^{a,b}

^aState Key Laboratory of Organic Geochemistry, Guangzhou Institute of Geochemistry, Chinese Academy of Sciences, Guangzhou 510640, China

^bUniversity of Chinese Academy of Sciences, Beijing 100049, China

ARTICLE INFO

Article history:

Received 30 August 2017

Received in revised form 20 November 2017

Accepted 3 January 2018

Available online 2 February 2018

Keywords:

Solid bitumen
Oil composition
Carbon isotope
Oil cracking

ABSTRACT

Highly mature solid bitumen, a residue of oil cracking, is widespread in the lower Paleozoic paleo-oil reservoirs of southern China. Solid bitumen is not a simple, pure component, but rather a compositionally and structurally variable mixture of materials. This study investigated the formation of thermogenic solid bitumen and the effects of oil composition and reservoir environment. A series of seven gold-tube pyrolysis experiments were conducted: three used the main fraction groups (i.e., saturated, aromatic, and resin + asphaltene fractions) of crude oil to evaluate the effect of oil composition on the formation of solid bitumen during cracking; the other four tested the effects of water and pressure in reservoirs by simulating the cracking of crude oil under different reservoir conditions. Quantitative analyses of pyrolytic products (including methane, C₂–C₅ gaseous hydrocarbons, C₆–C₁₃ light hydrocarbons, C₁₃₊ heavy hydrocarbons, and solid bitumen) indicated that thermogenic solid bitumen formed at different stages of oil cracking, and its formation was clearly affected by oil composition. In contrast, water and pressure in the reservoir had little effect on the formation of solid bitumen.

© 2018 Elsevier Ltd. All rights reserved.

1. Introduction

The lower Paleozoic of southern China has generally experienced deep burial, high thermal maturation, and intense tectonic activity. Its paleo-oil reservoirs therefore commonly contain highly mature solid bitumen (also termed “pyrobitumen” or “coke”) as a residue of oil cracking (Li et al., 2005; Ma et al., 2008; Liao et al., 2015). The destruction of crude oil components in these paleo-oil reservoirs as a result of cracking makes it difficult to correlate oil and gas sources. Solid bitumen preserved in paleo-oil reservoirs and migration pathways has experienced the entire process of thermal maturation, meaning that variations in its physical and chemical properties could provide insights into the evolution of the hosting reservoir. Therefore, the amount and distribution of solid bitumen could be used to delineate the range of paleo-reservoirs and further assess the scale of paleo-oil reservoirs and oil-cracked gas reservoirs (Zhao et al., 2006; Wang et al., 2007; Xiong et al., 2016).

However, the formation of solid bitumen during oil cracking is dynamic: its yield and characteristics change with thermal maturity and are possibly also influenced by other factors. Therefore, the use of indices (e.g., yield and the $\delta^{13}\text{C}$ values) based on solid bitumen simulating geological conditions is not simple, and a

number of issues must be addressed. First, thermal alteration is important to the formation of highly mature solid bitumen (Hwang et al., 1998). Pyrobitumen formation has been suggested to start during resin and asphaltene cracking (Horsfield et al., 1992; Schenk et al., 1997). Our previous simulation experiments of oil cracking indicated that thermogenic solid bitumen emerged mainly during the dry gas-generation stage of oil cracking (corresponding to 2.0–3.5% EasyRo); its maximum yield reached about 42% (by weight of oil) for a normal marine oil from the Tarim Basin (Xiong et al., 2016). Second, previous studies have shown that the oil composition within a reservoir possibly influences the formation and characteristics of solid bitumen (Nandi et al., 1978; Ungerer et al., 1988; Hill et al., 2003; Xiong et al., 2016). For example, asphaltenes and deasphalted heavy oils in Athabasca bitumen can produce structurally different cokes (Nandi et al., 1978). In addition to polar materials within oil, saturated and aromatic hydrocarbon fractions are possible precursors of pyrobitumen (Xiong et al., 2016). Aromatic oils can generate more pyrobitumen than paraffinic oils (Ungerer et al., 1988), and the aromatic content of oil can control the pyrobitumen yield of cracking (Hill et al., 2003). Given the complexity of crude oil mixtures, various secondary alterations, such as thermal alteration, biodegradation, and gas-washing, could change their composition. In addition, tectonic uplift might cause the pressure to drop in an oil reservoir, resulting in the migration of oil and gas and the deposition of

* Corresponding author.

E-mail address: xiongyq@gig.ac.cn (Y. Xiong).

asphaltenes due to a decrease in solvent capacity (Trindade et al., 1996).

This study employed a simplified crude oil mixture containing a limited number of saturated, aromatic, resin, and asphaltene fractions to assess quantitatively the effects of diverse oil components on the formation of solid bitumen. Three series of anhydrous pyrolysis experiments were performed at 50 MPa on three main group fractions (i.e., saturated, aromatic, and resin + asphaltene) of crude oil to evaluate their solid bitumen generation. Further thermal simulation experiments tested the effects of the reservoir environment by comparing the effects of the presence or absence of water and three different pressures (25, 75, and 100 MPa). This study would be useful in predicting the formation of thermogenic solid bitumen and its main characteristics, thereby providing key insights into the evaluation of oil-cracked gas resources in China.

2. Samples and experiments

2.1. Pyrolysis experiments

This study tested a sample of Tarim oil (as used by Xiong et al., 2016). The oil was first separated into saturated, aromatic, resin, and asphaltene fractions by asphaltene precipitation and column chromatography. Its group composition was 53.1% saturates, 16.0% aromatics, 15.4% resins, 3.86% asphaltenes, and 12% other components (water, insoluble minerals, volatilize light hydrocarbons, etc.). The four fractions were then dried at 50 °C. The low content of asphaltene was combined with resin as a polar fraction. Therefore, three fractions (saturated, aromatic, and resin + asphaltene) were considered in the following pyrolysis experiments. The oil group fractions were first pyrolyzed in a confined gold-tube anhydrous pyrolysis system (Xiong et al., 2016). Briefly, 10–30 mg of each group fraction was loaded into a series of gold tubes (length 40 mm; inner diameter 5 mm; wall thickness 0.5 mm). The tubes were then purged with argon for 5 min before being sealed under an argon atmosphere. The sealed tubes were placed in stainless steel autoclaves, and heated in an oven at a rate of either 20 or 2 °C/h at a constant pressure of 50 MPa, with 12 sampling temperature points designated between 330 and 600 °C for each heating rate. The autoclaves were removed from the oven after heating, and cooled in air. The thermal maturity of each sampling point was expressed using the equivalent vitrinite reflectance, EasyRo, as suggested by Sweeney and Burnham (1990).

To understand the effects of pressure and water on the formation of thermogenic solid bitumen, three complementary pyrolysis series were conducted at 25, 75, and 100 MPa, and a hydrous pyrolysis series was tested at 50 MPa for the whole oil. Anhydrous pyrolysis of the whole oil was performed previously by Xiong et al. (2016).

2.2. Determination of pyrolytic products

The chemical and carbon isotopic compositions of C₁–C₅ gaseous hydrocarbons (C₁–C₅ GHs) within the pyrolysates were determined by gas chromatography (GC) and GC–isotope ratio mass spectrometry (GC–IRMS). After pyrolysis, each gold tube was cleaned, weighed (using a Sartorius CPA225D electronic balance, ±0.01 mg below 100 g), and placed in a vacuum glass system connected to the GC inlet. The tube was then pierced using a steel needle, releasing the gaseous products into the GC system (Agilent Technologies 7890-0322) for quantification. The refinery gas analyzer included two thermal conductivity detectors for the analysis of permanent gases and a flame ionization detector for the analysis of hydrocarbon gases, as well as five rotary valves and seven columns. This enabled the analysis of all gaseous components with

a single injection. Carbon isotopic composition was determined using a stable isotope mass spectrometer (GV Instruments Iso-prime). The gas chromatograph (Agilent 6890) was equipped with a capillary column (HP-PLOT Q, 30 m × 0.32 mm × 20 mm) with helium as the carrier gas. The oven temperature was programmed by 50 °C for 3 min before being heated to 190 °C at a rate of 25 °C/min and then held isothermally for 8 min. Carbon isotope ratios for individual hydrocarbons were calculated using CO₂ as a reference gas that was automatically introduced into the IRMS system at the beginning and end of each analysis. The data are reported in per mil (‰) relative to the VPDB standard.

After the analysis of C₁–C₅ GHs, the pierced gold tube was dried at 50 °C in an electric vacuum drying oven to evaporate volatile C₆–C₁₃ light hydrocarbons (LHs), until the weight of the tube remained constant. Comparison of the weight loss during the analysis of C₁–C₅ GHs and inorganic gases (e.g., CO₂, H₂, and O₂) with the total mass of C₁–C₅ GHs, LHs, and inorganic gases generated during pyrolysis could thus obtain the yield of LHs by subtraction.

After determining the mass of the LHs, the weighed gold tube was cut in half, placed in a 4 mL sample vial of dichloromethane, and ultrasonicated for 30 min to accelerate the dissolution of C₁₃₊ heavy hydrocarbons (HHs). It was then rested for 12 h. The solution was filtered before being evaporated to constant weight to determine the weight of the soluble HHs fraction. The mass of solid bitumen was finally obtained by subtraction (i.e., the total oil weight less the sum of the measured weights of C₁–C₅ GHs, inorganic gases, LHs, and HHs) given mass conservation. The mass of solid bitumen has previously been obtained by direct weighing of the filtered residue (Xiong et al., 2016). The results of the two methods are compared and discussed in Section 3.3. The δ¹³C value of solid bitumen was determined using GC–IRMS (Thermo Finigan Delta Plus XL).

3. Results and discussion

3.1. Pyrolytic characteristics of fractions in crude oil

To better depict the pyrolytic characteristics of the three different oil fractions (saturated, aromatic, resin + asphaltene), the pyrolytic products were subdivided into five main types according to the analytic methods: methane (C₁), C₂–C₅ GHs, volatile C₆–C₁₃ LHs, solvable C₁₃₊ HHs, and solid bitumen. Fig. 1 shows the variations in these components in the pyrolytic products during the cracking of the three different fractions. Four stages of oil cracking have been established for this pyrolysis system (Fang et al., 2012; Xiong et al., 2016); the four stages of thermal maturity used to identify the thermal maturation are the oil-generation stage (Stage I, corresponding to 0.5–1.0% EasyRo), the condensate-generation stage (Stage II, 1.0–1.5% EasyRo), the wet gas-generation stage (Stage III, 1.5–2.2% EasyRo), and the dry gas-generation stage (Stage IV, >2.2% EasyRo).

As shown in Fig. 1, at the beginning of pyrolysis the saturated fraction consists of LHs (34%) and HHs (66%), while the aromatic and resin + asphaltene fractions have similar initial constituents: LHs (11%) and HHs (89%). With increasing thermal maturity, the content of HHs rapidly decreases in the EasyRo range of about 0.8–2.2%; it then slowly decreases after entering the dry gas-generation stage, before disappearing at ~4.0% EasyRo. The content of LHs first increases with maturity during Stages I and II, and reaches a maximum value of about 64.6% (saturated fraction), 33.7% (aromatic fraction), and 29.5% (resin + asphaltene fraction) at 1.5% EasyRo, but subsequently decreases. The aromatic and resin + asphaltene fractions show very similar evolution curves to C₁ and C₂–C₅ GHs. The C₂–C₅ GHs gradually increase within the EasyRo range of 1.0–2.2% (Stages II and III), reaching a maximum

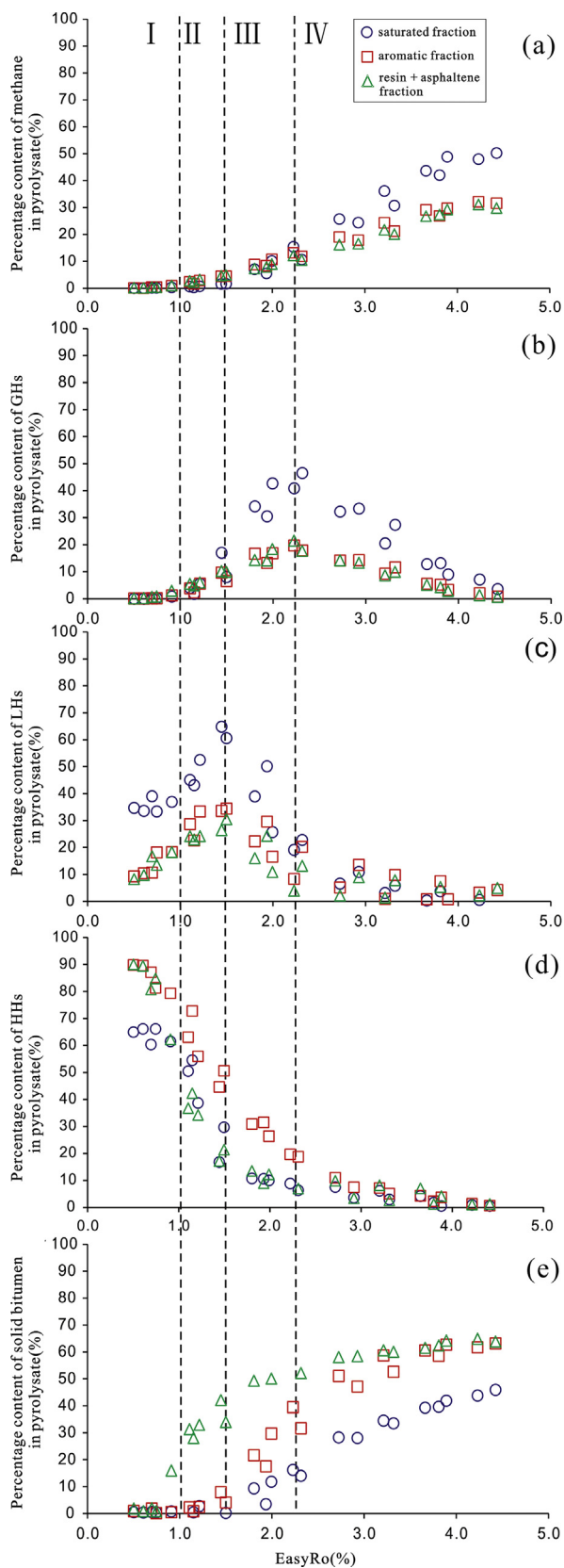


Fig. 1. Variations in the percentage contents of (a) C_1 , (b) C_2 – C_5 GHs, (c) C_6 – C_{13} LHs, (d) C_{13+} , HHs, and (e) solid bitumen in pyrolysates during the thermal treatment of different fractions. I – oil-generation stage (corresponding to 0.5–1.0% EasyRo), II – condensate-generation stage (corresponding to 1.0–1.5% EasyRo), III – wet gas-generation stage (corresponding to 1.5–2.2% EasyRo), and IV – dry gas-generation stage (corresponding to >2.2% EasyRo).

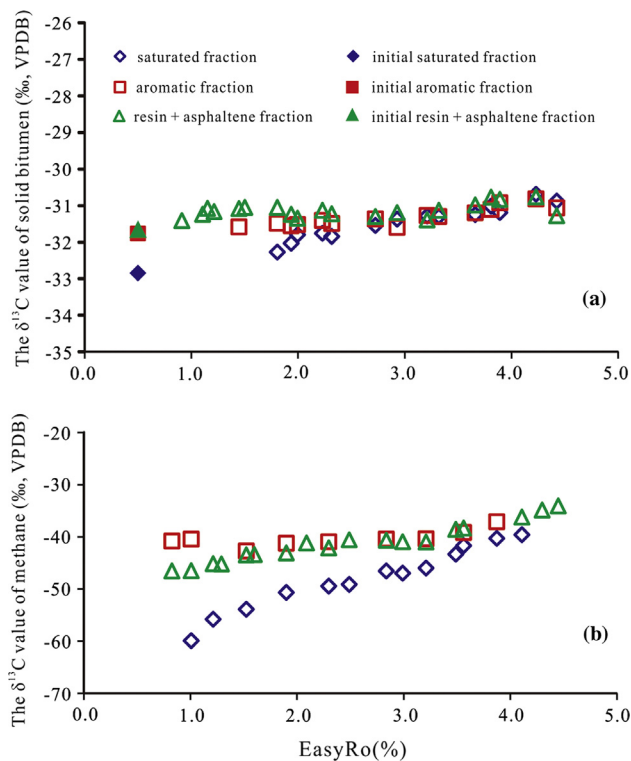


Fig. 2. $\delta^{13}C$ curves of (a) solid bitumen and (b) methane generated from saturated, aromatic, and resin + asphaltene fractions during thermal treatment.

content of 20% at 2.2% EasyRo before gradually decreasing as EasyRo further increases to 4.5% (Stage IV). The methane content increases from 4.6% at 1.5% EasyRo to 29.5% at 4.0% EasyRo. Methane and C_2 – C_5 GHs from the saturated fraction also have similar content curves to those of the aromatic and resin + asphaltene fractions, but with the difference of reaching higher maximum contents (50.2% and 46.4%, respectively) than the latter two fractions.

The solid bitumen generation curves of the different group fractions are obviously different (Fig. 1). Solid bitumen from the aromatic fraction is generated mainly within 1.5–3.2% EasyRo, reaching a maximum content of 58.6% at ca. 3.2% EasyRo, while its generation from the resin + asphaltene fraction begins earlier (EasyRo ~ 0.8%) and then rapidly increases up to 51% at 2.2% EasyRo before slowly increasing to a maximum yield of 60.6% at 3.2% EasyRo. The formation of solid bitumen from the saturated fraction begins at 1.5% EasyRo and gradually increases to 45.9% at 4.5% EasyRo.

Overall, the aromatic and resin + asphaltene fractions are rich in HHs. Most of the HHs in the resin + asphaltene fraction are transformed to solid bitumen during condensate generation and wet gas generation (Stages II and III); the transformation of HHs in the aromatic fraction to solid bitumen mainly occurs in Stage III and early Stage IV. However, HHs in the saturated fraction initially generate LHs and C_1 – C_5 GHs during Stages I and II, and then solid bitumen is produced mainly in Stages III and IV, derived from the cracking of LHs and C_2 – C_5 GHs.

3.2. $\delta^{13}C$ of methane and solid bitumen in pyrolysates

In highly overmature regions, the $\delta^{13}C$ values of methane and solid bitumen are useful indicators of the origin and source of natural gases. Therefore, it is necessary to understand their evolution during thermal maturation and the main influencing factors to

explain data from actual gas reservoirs. Fig. 2 presents $\delta^{13}\text{C}$ profiles of methane and solid bitumen generated from the different fractions of the present study during thermal maturation. The $\delta^{13}\text{C}_1$ trends in Fig. 2b demonstrate that methane generated from all fractions is depleted in ^{13}C relative to its precursors; e.g., the initial $\delta^{13}\text{C}$ values of the saturated, aromatic, and resin + asphaltene fractions used for pyrolysis experiments are -32.8‰ , -31.8‰ , and -31.7‰ , respectively (Fig. 2a). Methane from the saturated fraction is especially depleted in ^{13}C (about 27‰) at the beginning of formation, but then displays ^{13}C enrichment with maturity, with $\delta^{13}\text{C}_1$ varying from -59.9‰ to -39.6‰ . Methane derived from the aromatic fraction has a relatively constant carbon isotope content, with $\delta^{13}\text{C}_1$ values of -42.7‰ to -39.2‰ . Methane from the resin and asphaltene fraction shows a similar carbon isotope trend, with just a slight depletion of ^{13}C occurring between 0.8% and 1.5% EasyRo.

In contrast, solid bitumen generated by the different components in crude oil is relatively enriched in ^{13}C compared with the initial reactants. It has largely stable $\delta^{13}\text{C}$ values ($-31.5\text{‰} \pm 0.5\text{‰}$) during the main formation stage, although solid bitumen from the saturated fraction is slightly depleted in ^{13}C during the initial stage (1.8–2.0% EasyRo) (Fig. 2a). It has been suggested that solid bitumen is formed via aromatic condensation reactions (Ungerer et al., 1988; Behar et al., 1992; Hill et al., 2003) that involve insignificant carbon isotopic fractionation. Therefore, the $\delta^{13}\text{C}$ value of solid bitumen preserved in paleo-oil reservoirs is indicative of the $\delta^{13}\text{C}$ value of the source rocks, thus enabling bitumen to be correlated with its source rock.

3.3. Effect of oil composition on the formation of solid bitumen

Previous cracking simulation experiments have shown that aromatic-rich Boscan oil and saturate-rich Pematang oil produced pyrobitumen with yields of 41 wt.% and 24 wt.%, respectively, at EasyRo 2.0% (450 °C, heating time 7 h) (Ungerer et al., 1988). The pyrolysis of saturate-rich Devonian oil from the Western Canada Sedimentary Basin has also yielded a significant amount of pyrobitumen (about 40%) at EasyRo 2.83% (Hill et al., 2003), indicating that oil composition has an important influence on the formation of solid bitumen.

From the composition of the present oil (Section 2.1) and the solid bitumen yield curves of the different fractions (Fig. 1e), the

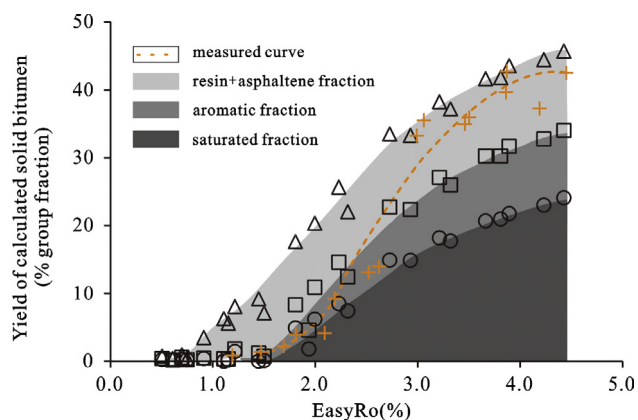


Fig. 3. Measured and calculated yield curves of solid bitumen generated during oil cracking. The measured data are from Xiong et al. (2016). ○ – the yield of solid bitumen derived from the saturated fraction at a certain maturity; □ – the yield of solid bitumen derived from saturated + aromatic fractions at a certain maturity; △ – the yield of solid bitumen derived from saturated + aromatic + resin + asphaltene fractions at a certain maturity; + – the yield of solid bitumen derived from crude oil at a certain maturity (data from Xiong et al., 2016).

solid bitumen yield of the whole oil at a certain maturity level can be calculated from the curves in Fig. 3. The calculated curves for solid bitumen yield (Fig. 3) show that the solid bitumen formed at ~ 0.5 –1.5% EasyRo is derived mainly from the cracking of the resin + asphaltene fraction; its yield at 1.5% EasyRo reached about 9.2% of the maximum yield. Therefore, most solid bitumen is accumulated from the cracking of saturated and aromatic fractions, whereas almost no solid bitumen is generated from the resin + asphaltene fraction at $>1.5\%$ EasyRo. This indicates that the content of resin and asphaltene fractions in oil controls the yield of solid bitumen in the main oil-generation stage, while the content of saturated and aromatic fractions governs the formation of solid bitumen at $>1.5\%$ EasyRo. The calculated maximum yield of solid bitumen reaches 45.7% of the original mass of the oil at 4.5% EasyRo (Fig. 3), which is close to the solid bitumen yield (about 42% at 4.5 EasyRo) of the crude oil measured by Xiong et al. (2016). Approximately 52% of the maximum yield is generated from the saturated fraction, 22% from the aromatic fraction, and 26% from the resin + asphaltene fraction. Thus, if the proportion of different components in crude oil were known, the solid bitumen yield curve during oil cracking could be estimated based on these results.

A significant difference between the solid bitumen yield calculated here from the mass balance and that previously measured (Xiong et al., 2016) occurs at maturities of $<1.5\%$ EasyRo (Fig. 3). The difference is mainly attributable to the formation of solid bitumen from the resin + asphaltene fraction during the oil-generation stage. The indirect method of solid bitumen calculation used here might be more accurate than the previous method of direct weighing, because any small bitumen mass loss (e.g., during extraction and washing) can lead to large errors in the result owing to the minor production of solid bitumen at $<1.5\%$ EasyRo. However, at high maturity ($>2.2\%$ EasyRo), the results of the two methods are similar as the production of solid bitumen is relatively high, lessening the effect of any bitumen mass loss.

3.4. Effects of water and pressure on the formation of solid bitumen

In addition to thermal maturity, water and pressure can also possibly influence oil cracking in the lower Paleozoic paleo-oil reservoirs of southern China. Hill et al. (2003) suggested that increased pressure does not affect the reaction mechanisms of oil cracking; however, cracking is slightly enhanced below 60–70 MPa and impeded at >60 –70 MPa (Hill et al., 1996).

This study compares oil cracking and the formation of solid bitumen under different environments: hydrous versus anhydrous and at different pressures (25, 50, 75, and 100 MPa). Overall, the production of solid bitumen does not vary greatly under these different conditions (Fig. 4): it begins at EasyRo $\sim 1.5\%$, rapidly increases between 2.0% and 3.5% EasyRo, and slowly increases up to 4.0% EasyRo, suggesting that pressure and water have no remarkable effect on the formation of solid bitumen.

These are preliminary results of our study where thermal cracking of a pure oil and its oil fractions were simulated to quantitatively assess and predict the formation of solid bitumen during oil cracking. However, the experimental conditions are simplified and differ in some ways from actual geological circumstances of reservoirs and source rocks. For instance, minerals in sedimentary rocks, such as CaCO_3 , CaSO_4 , pyrite, quartz, and acidic clays can change the chemical composition and yield of oil generated from hydrous pyrolysis of either kerogens or source rocks (Horsfield and Douglas, 1980; Davis and Stanley, 1982; Tannenbaum et al., 1986; Taulbee and Seibert, 1987; Lao et al., 1989; Siskin and Katritzky, 2001;) and may affect the formation of solid bitumen. Additionally, the catalytic effects of minerals on the cracking of oils depend on the direct contact of oils with mineral surfaces in rocks

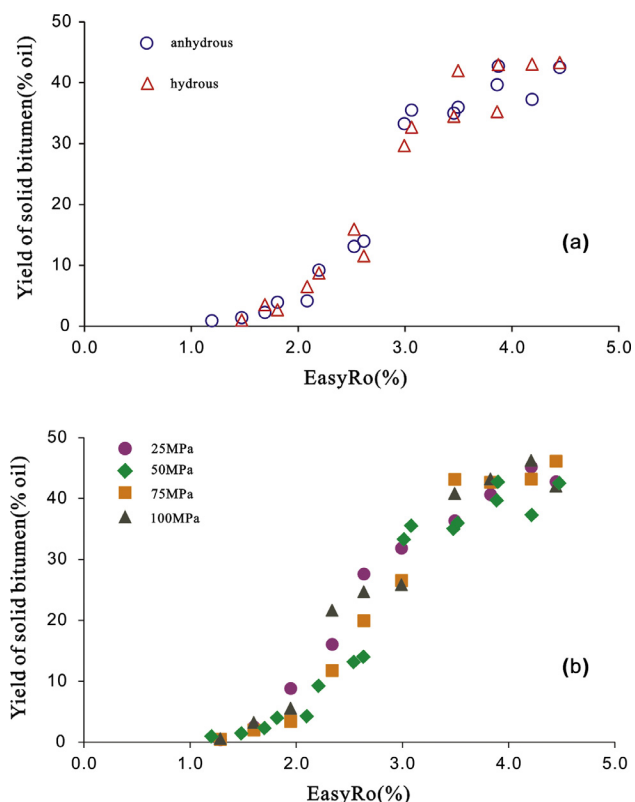


Fig. 4. Yield curves of solid bitumen under different conditions: (a) anhydrous vs. hydrous; (b) pressures of 25, 50, 75, and 100 MPa.

(Pepper and Dodd, 1995). Future work should examine such effects by performing hydrous pyrolysis experiments of both crushed and uncrushed source rock fragments on the generation of solid bitumen. Various factors, such as, reservoir lithology (sand, clay, carbonate, etc.), oil types (marine, terrestrial, and coal-derived oils), and water, etc., should also be taken into consideration in the future work.

4. Conclusions

This study aimed to elucidate the main factors influencing the formation of thermogenic solid bitumen. Pyrolysis experiments on different fractions and under different reservoir conditions led to the following main conclusions.

- (1) Different fractions in oil have distinct capacities of solid bitumen generation and different main stages of formation. For example, solid bitumen from saturated and aromatic fractions emerges mainly in Stages III and IV of oil cracking (saturated fraction: 1.5–4.5% EasyRo; aromatic fraction: 1.5–3.5% EasyRo), and the maximum yields of these fractions are 45.9% and 58.6%, respectively. In contrast, solid bitumen sourced from the resin + asphaltene fraction is generated mainly in Stages I and II (0.8–1.5% EasyRo), and its maximum yield is 60.6%. These results indicate that oil composition is a critical factor controlling the formation and yield of solid bitumen during oil cracking.
- (2) The $\delta^{13}\text{C}$ values of solid bitumen generated by different fractions of crude oil are relatively constant (i.e., $-31.5\text{‰} \pm 0.5\text{‰}$) during thermal maturation, and are slightly more positive than those of the initial aromatic and resin + asphaltene fractions. Therefore, the $\delta^{13}\text{C}$ value of solid bitumen preserved in paleo-oil reservoirs can be used to identify its source rock.

- (3) Water and pressure in reservoirs appear to have no remarkable effect on the formation of solid bitumen. All yield curves follow similar trends; i.e., solid bitumen first forms at EasyRo $\sim 1.5\%$, rapidly increases between 2.0% and 3.5% EasyRo, and then slowly increases up to a maximum at 4.0% EasyRo.

Acknowledgements

This work was financially supported by Special Fund for Strategic Priority Research Program of the Chinese Academy of Sciences (Class B) (Grant No. XDB10010500), GIGCAS 135 Project (Grant No. 135TP201602), National Science and Technology Major Project of the Ministry of Science and Technology of China (Grant No. 2017ZX05008-002-020) and National Natural Science Fund of China (Grant No. 41672126). We also acknowledge Editor in Chief Erdem Idiz, Associate Editor Andrew Murray and the two anonymous reviewers for their helpful comments and suggestions.

Associate Editor—Andrew Murray

References

- Behar, F., Kressmann, S., Rudkiewicz, J.L., Vandenbroucke, M., 1992. Experimental simulation in a confined system and kinetic modelling of kerogen and oil cracking. *Organic Geochemistry* 19, 173–189.
- Davis, J.B., Stanley, J.P., 1982. Catalytic effect of smectite clays in hydrocarbon generation revealed by pyrolysis-gas chromatography. *Journal of Analytical and Applied Pyrolysis* 4, 227–240.
- Fang, C., Xiong, Y., Liang, Q., Li, Y., 2012. Variation in abundance and distribution of diamondoids during oil cracking. *Organic Geochemistry* 47, 1–8.
- Hill, R.J., Tang, Y., Kaplan, I.R., 2003. Insights into oil cracking based on laboratory experiments. *Organic Geochemistry* 34, 1651–1672.
- Hill, R.J., Tang, Y., Kaplan, I.R., Jenden, P.D., 1996. The influence of pressure on the thermal cracking of oil. *Energy and Fuels* 10, 873–882.
- Horsfield, B., Douglas, A.G., 1980. The influence of minerals on the pyrolysis of kerogens. *Geochimica et Cosmochimica Acta* 44, 1119–1131.
- Horsfield, B., Schenk, H.J., Mills, N., Welte, D.H., 1992. An investigation of the in-reservoir conversion of oil to gas: compositional and kinetic findings from closed-system programmed-temperature pyrolysis. *Organic Geochemistry* 19, 191–204.
- Hwang, R.J., Teerman, S.C., Carlson, R.M., 1998. Geochemical comparison of reservoir solid bitumens with diverse origins. *Organic Geochemistry* 29, 505–517.
- Lao, Y., Korth, J., Ellis, J., Crisp, P.T., 1989. Heterogeneous reactions of 1-pristene catalyzed by clays under simulated geological conditions. *Organic Geochemistry* 14, 375–379.
- Li, J., Xie, Z., Dai, J., Zhang, S., Zhu, G., Liu, Z., 2005. Geochemistry and origin of sour gas accumulations in the northeastern Sichuan Basin, SW China. *Organic Geochemistry* 36, 1703–1716.
- Liao, Y., Fang, Y., Wu, L., Cao, Q., Geng, A., 2015. The source of highly overmature solid bitumens in the Permian coral reef paleo-reservoirs of the Nanpanjiang Depression. *Marine and Petroleum Geology* 59, 527–534.
- Ma, Y., Zhang, S., Guo, T., Zhu, G., Cai, X., Li, M., 2008. Petroleum geology of the Puguang sour gas field in the Sichuan Basin, SW China. *Marine and Petroleum Geology* 25, 357–370.
- Nandi, B.N., Belinko, K., Ciavaglia, L.A., Pruden, B.B., 1978. Formation of coke during thermal hydrocracking of Athabasca bitumen. *Fuel* 57, 265–268.
- Pepper, A.S., Dodd, T.A., 1995. Simple kinetic models of petroleum formation. Part II: oil-gas cracking. *Organic Geochemistry* 12, 321–340.
- Schenk, H.J., Diprimio, R., Horsfield, B., 1997. The conversion of oil into gas in petroleum reservoirs. Part 1: comparative kinetic investigation of gas generation from crude oils of lacustrine, marine and fluviodeltaic origin by programmed-temperature closed-system pyrolysis. *Organic Geochemistry* 26, 467–481.
- Siskin, M., Katritzky, A.R., 2001. Reactivity of organic compounds in superheated water: general background. *Chemical Reviews* 101, 825–835.
- Sweeney, J.J., Burnham, A.K., 1990. Evaluation of a simple model of vitrinite reflectance based on chemical kinetics. *American Association of Petroleum Geology Bulletin* 74, 1559–1570.
- Tannenbaum, E., Ruth, E., Kaplan, I.R., 1986. Steranes and triterpanes generated from kerogen pyrolysis in the absence and presence of minerals. *Geochimica et Cosmochimica Acta* 50, 805–812.
- Taulbee, D.N., Seibert, E.D., 1987. Comparison of the hydrocarbon pyrolysis products from a Devonian type II kerogen to those from kerogen/mineral blends. *Energy and Fuels* 1, 514–519.

- Trindade LAF, Philp RP, Mizusaki AMP, des Santos RL, Tchouparova AE, Djafarian MS. Geochemical characterization of waxy oils from the Dom Juao oil field, Reconcavo Basin, Brazil. In: Proceedings of the 5th Latin American organic geochemistry congress, Cancun, Mexico; 1996. p. 281–3.
- Ungerer, P., Behar, F., Villalba, M., Heum, O.R., Audibert, A., 1988. Kinetic modelling of oil cracking. *Organic Geochemistry* 13, 857–868.
- Wang, T., Geng, A., Xiong, Y., Geng, X., 2007. Mass balance calculation of the pyrolysates generated from marine crude oil: a prediction model of oil cracking gas resources based on solid bitumen in reservoir. *Chinese Science Bulletin* 52, 1532–1539.
- Xiong, Y., Jiang, W., Wang, X., Li, Y., Chen, Y., Zhang, L., et al., 2016. Formation and evolution of solid bitumen during oil cracking. *Marine and Petroleum Geology* 78, 70–75.
- Zhao, W., Wang, Z., Wang, Y., 2006. Formation mechanism of highly effective gas pools in the Feixianguan Formation in the NE Sichuan Basin. *Geological Reviews* 52, 708–717.